PREDICTIVE UNCERTAINTY ESTIMATES IN GEOTHERMAL RESERVOIR MODELS USING LINEAR ANALYSIS

Jericho Omagbon[1/2], Michael O'Sullivan[2], John O'Sullivan[2] and Cameron Walker[2]

[1] Energy Development Corporation, One Corporate Centre Building, Ortigas Center, Pasig City, Philippines

[2] Department of Engineering Science, The University of Auckland, 70 Symonds Street, Auckland, New Zealand

omagbon.jb@energy.com.ph

Keywords: *Sensitivity, parameter estimation, uncertainty analysis, reservoir modelling, PEST, Monte Carlo, linear analysis.*

ABSTRACT

Deterministic simulation models of geothermal systems are now used extensively, not only to understand the different processes occurring within the geothermal reservoir, but also to predict future responses. Accurate model results are critical for the short- and long-term management of a geothermal field, particularly in determining the production strategy and ongoing management and development of the field. However, model predictions are often affected by uncertainties in input data, model parameters, and by incomplete knowledge of the underlying physics. A deterministic simulation assumes one set of input conditions, and generates one result without considering uncertainties. When making decisions based on these models, managers of geothermal fields must include some estimate of uncertainty to reflect the imperfect information at their disposal. In this work, we present a method for estimating the uncertainty in the prediction of a reservoir model, thus taking an important step towards the development of a more robust decision support tool.

A synthetic 2D model that included six faults was developed and then used to generate production data against which the working model could be calibrated. Calibration was carried out using the gradient based Levenberg Marquardt optimization algorithm with Tikhonov regularization. The calibration process determined the possible parameter values for the faults and background permeability of the working model using temperature, pressure and tracer recovery curves. Assuming a parameter probability distribution based on the result of the local sensitivity information at the optimum parameter values, a Monte Carlo analysis was then used to investigate the uncertainty interval of the model prediction of four different forecast scenarios.

1. INTRODUCTION

A numerical model of a geothermal system enables forecasts to be made of its response to different operating scenarios. With these forecasts, different resource management strategies can be explored and compared, allowing an optimal decision to be made. This requires that the properties of the numerical model are consistent with that of the real-life system. This is obviously very difficult to achieve for several reasons. One reason for this difficulty is that physical reservoir properties, boundary conditions and geological parameters are very difficult if not impossible to measure accurately in the field at a resolution that would be useful in the model. Another reason is the governing equations used to calculate the state of the system are approximate. The level of approximation gets worse when computational constraints are taken into account as these tends to force the modeller to reduce the resolution of the model to be able to complete the computations within a reasonable amount of time.

In place of directly measuring system properties, modellers employ calibration in order to estimate the important reservoir properties which they think affect the field behaviour of interest. This is achieved by comparing a model response with responses measured from the real system such as downhole logs and well flow data, as well as making use of the modeller's prior knowledge about the other aspects of the conceptual model of the system. The ultimate goal of using the model to make different forecasts can then be performed once these important parameters that control the response of the system have been identified.

The traditional way that models are used in the geothermal industry is to make reservoir development or resource management decisions using production forecasts from one version of a history matched model. Often several scenarios are investigated and compared with each other. The one which has the most benefit from a financial, technical or environmental perspective is then chosen from these different forecast scenarios. However, no matter how well a calibrated model fits the measured data, it does not necessarily represent the true behaviour of a real system because of the complexities inherent in the system being modelled. This is an obvious result of the limitation of the parameters that can be measured in the field. Consequently, any prediction made on the basis of the calibrated model has a potential error. Such an error must therefore be accounted for when making resource management decisions on the basis of model outcomes.

This work investigates methods for quantifying uncertainty in a geothermal reservoir simulation. To characterize the uncertainty in predicted reservoir performance, it should be first recognized that numerical models are inherently non-unique and there exists several different sets of model structure and/or parameters that can describe a real system. The problem therefore translates to finding different sets of reservoir descriptions that honour all available data so that they can be used to simulate reservoir performance. The data that must be honoured includes both expert knowledge and measured quantities. Sampling methods are proposed to generate these different realizations of the model that behave like the real system. The outcome of this work will contribute to improving the geothermal modelling practice with respect to quantifying prediction uncertainties so that model results can be better interpreted and used as a resource management tool. The information about the uncertainties involved in the model provides a confidence level about the model forecast which can assist the geothermal operators in assessing the risks involved in using the model results and in making decisions accordingly.

1.1 Brief review of previous work on uncertainty quantification of geothermal model predictions

Three notable studies on this topic have been reported in the literature. Tureyen & Onur (2010) presented an uncertainty quantification study of a lumped-parameter problem using the pressure data from the Balcova-Narlidere geothermal field. They used a randomized maximum likelihood method to generate several realizations of the model parameters that can reproduce the measured pressure. In the method that they used, several random sets of parameter values were generated. The parameter values in each of the generated sets of samples are then adjusted so that the model response is consistent with the measured pressure. The predictive uncertainty is then characterized by obtaining predictions from each of the model realizations.

Vogt, *et. al*. (2012) estimated the uncertainty in the long term performance prediction of the model for the Soultz EGS project. They used sequential Gaussian simulation to generate 880 model realizations. The permeability structure of each realization was calibrated using an Ensemble Kalman Filter to fit their response to the measured temperature and pressure logs as well as tracer circulation data. Finally, the ensemble of calibrated models obtained during the calibration stage was used to estimate the uncertainty in the 50 year prediction of the variation in head and temperature within the reservoir.

A more recent uncertainty estimation study was made by Moon, *et al.* (2014) using a model of the Ngatamariki geothermal system. In their work, they explored the uncertainties in the forecasted enthalpies of a 50 year production forecast. They identified the key parameters in the model that affected the natural state behaviour and the prediction of interest by ranking their influences based on the normalized sensitivity coefficients. Using the estimated value as the mean and assigned ranges as the basis for the uncertainty, they generated random samples of these highly influential parameters to generate different model realizations. With the generated samples, they were able to propagate the uncertainties of the selected parameters to the forecasted enthalpies in the production wells.

2. DESCRIPTION OF THE METHODOLOGY

One method of estimating the uncertainty is to generate all the models that are consistent with both the measured data and conceptual information of the system, and then simulate future production using each of them. In the geothermal modelling context, this is a difficult task because the time needed to obtain each calibrated model can typically be several months or even a few years. Uncertainty quantification is even more computationally expensive because of the need to generate a sufficiently large number of these calibrated models to properly characterize the uncertainty. In this work, an alternative two-step process of generating several samples of near-calibrated models is considered. The steps involved are (1) calibrating the model, then (2) generating samples using information from the calibration process to carry out the error analysis. The general approach is similar to that used by Moon, *et al.* (2014) with some notable differences. First, the parameter uncertainties are based on how well the parameter values were identified during the calibration process rather than being assigned a priori. Second, the propagation of uncertainty is not limited to a few selected influential parameters. Third, a much larger number of Monte Carlo samples were made to ensure a reasonable coverage of the parameter space.

The method used is linear perturbation analysis. This method has been described by several other authors (Press, *et. al*., 1996), (Finsterle, 1999), (Tarantola, 2005), (Oliver, Reynolds, & Liu, 2008) and (Doherty, 2015). It is based on the idea that once the values of the model parameters have been adjusted to obtain an acceptable match between the model response and the measured data, those parameter values can be perturbed slightly and the match obtained should still be acceptable. The same perturbation can then be applied to model predictive runs to obtain a range of possible outcomes. If the perturbation is sufficiently small, a linear analysis can be used to derive confidence intervals for a future prediction run. The perturbation in the parameter values can be obtained using the post calibration parameter uncertainty as a basis. This requires that the derivatives (gradients) of the response data with respect to the parameters in the model are known.

The method starts with the uncertainty propagation equation for a linear model given by (Arras, 1998):

$$\sigma^2 = J_0 C_x {J_0}^T \tag{1}$$

In this equation, σ^2 is a matrix with the number of rows and columns equal to the number of predicted quantities and whose diagonal elements corresponds to the variance of each predicted quantity. J_0 is the Jacobian matrix which is composed of elements defined by: $J_{0ij} = \frac{\partial y_{0i}}{\partial x_j}$, i.e., the gradient of predicted value y_{0i} with respect to all parameters x_j. The matrix C_x on the other hand is the variance-covariance matrix of parameter x which contains the parameter uncertainty and the correlation information for the parameters. For a well-posed inverse problem with parameters estimated by minimizing a least squares objective function to obtain small residuals (difference between model and measured data), this C_x matrix can be obtained using the equation:

$$C_x = (J^T W J)^{-1} \tag{2}$$

J in (2) is similar to J_0 in (1) except that the element J_{ij} here is the gradient of the calculated historical response (rather than the predicted quantity), with respect to all parameters x_j. W is the weighing matrix whose diagonal element is the inverse of the variance that represents the measurement error of the observation data that were used in the parameter estimation process. For a single prediction y_o with uncorrelated parameters, (1) takes the more familiar form (Devore, 1987):

$$\sigma(y_o)^2 = \sum_i \left(\frac{\partial y}{\partial x_i}\right)^2 (\sigma(x_i)^2) \tag{3}$$

Equation (3) implies that there are two factors affecting the uncertainty in the model prediction; (1) the sensitivity of the prediction with respect to the parameters and (2) the uncertainty in the parameter value. Thus, a highly uncertain parameter may not necessarily affect the prediction uncertainty if that parameter has small influence over the predicted quantity. Conversely, a parameter with small uncertainty may result to a high predictive uncertainty if the parameter has very high impact on the predicted quantity.

Geothermal models are typically nonlinear but they can be assumed to be linear near the minimum of the objective function by virtue of a first-order Taylor series approximation. The steps needed to quantify model prediction uncertainty based on the theory above are as follows:

i. Calibrate the model either manually or automatically using a minimization algorithm. This will put the model in a "low residuals" state to make (2) valid.

ii. Calculate the calibration gradient matrix *J* based on the best estimated parameters then use (2) to obtain the post-calibration variance-covariance matrix which contains the parameter uncertainty and correlation information. The gradient matrix *J* can be obtained through a finite difference approximation. Automatic parameter estimation software such as PEST and iTOUGH provides utilities to obtain both the gradient and covariance matrix.

iii. Monte Carlo simulation may be performed using the covariance matrix in Step (ii) as a basis for the probability distribution of the uncertain parameters. The sampling method used for the Monte Carlo analysis in this paper assumed a normal distribution for the uncertain parameters with mean and standard deviation based on the best parameter estimate and the post calibration parameter variance (from the covariance matrix), respectively. If the standard deviation for a certain parameter is unrealistically high, it must be replaced with a reasonable lower value that reflects expert knowledge. This will prevent sampling of extremely high or extremely low parameter values. To improve the efficiency, Latin hypercube sampling is used and the parameter correlation structure based on the post-calibration covariance matrix was imposed using the rank correlation method described by Iman & Conover (1982). A rejection criterion was added by setting a threshold objective function value to ensure that the distribution of models prediction only includes those which were considered to be in a near-calibrated state. The models which pass this acceptance test are used to make predictions.

3. APPLICATION TO A SYNTHETIC MODEL

A synthetically-generated 2D production-injection model was constructed with TOUGH2 to serve as the 'true' system. The model covers a total lateral area of 100km^2 and a thickness of 1000m. The model domain has a region with fine grid blocks 50m x 50m in size where three production wells and one injection well were placed. Outside this fine grid region, the blocks increase gradually up to a maximum size of 500m x 500m. The model starts off with uniform temperature and pressure of 270°C and 18 MPa, respectively. There were no upflow, outflow or heat fluxes defined. This was done mainly to simplify the problem and to do away with the need for a natural state run. There were pressure dependent recharge blocks at the edge of the model to prevent the pressure from continually dropping as fluid was extracted from the production wells.

The flow in the model is controlled by the six high permeability paths representing the faults and the non-uniform background permeability. The heterogeneous background permeability was generated by kriging interpolation from 200 arbitrary pilot points. The corresponding permeability values at each of the pilot points were sampled randomly from a normal distribution. The kriging interpolation used a spherical variogram that was fitted against the variogram of the 200 pilot points. The variogram has a maximum correlation length of 3000m and has no anisotropy. A dual porosity approach composing of 3 interacting continua (1 fracture and 2 matrix elements) was applied throughout the entire model domain in order to obtain good temperature and tracer recovery trends.

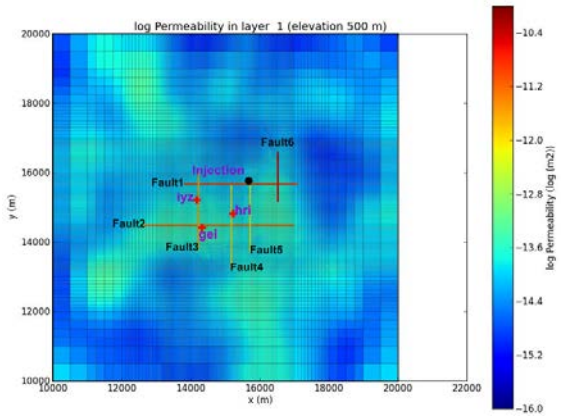

Figure 1. Synthetic model configuration. The red and blue dots are the production and injection wells location, respectively. The model has a non-uniform background permeability generated by kriging from 200 arbitrary pilot point locations.

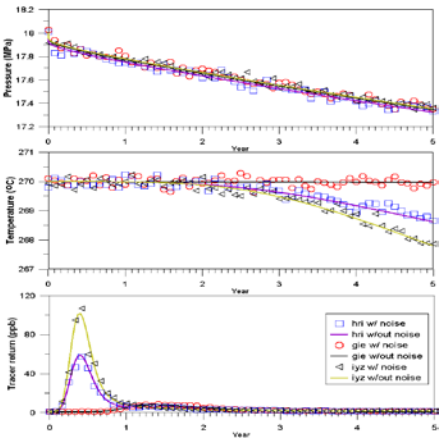

Figure 2. Measured data generated from the synthetic model

During the production period, the three production wells were set to produce at constant flow rates with a combined total of 180 kg/s. The injection well was set to a constant injection of 136 kg/s (~75 % of the produced fluid) at an injection temperature of 160°C. This production-injection scheme drives the response of the reservoir which was monitored through the temperature/enthalpy and pressure at the production wells. Tracer was also injected into the injection well at the start of production and the tracer return was monitored from the three production wells.

It was assumed that the reservoir had been operating under these conditions for the past 5 years. In a real geothermal field operation, the production and injection rates would have changed with time in response to pressure decline and cooling/boiling. However in the synthetic model, this effect has been left out since it is assumed that the injection and production rates are perfectly known in the working model. Synthetic calibration data representing the reservoir

response composed of the temperature, pressure and tracer concentration from each of the production wells was obtained by running this model for 5 years. Artificial noise was added to the simulated response.

3.1 Working Model Description

A model with a similar structure and dimensions to the synthetic or truth model was constructed to serve as the working model. It covers the same area, and has the same number and sizes of grid blocks. The fault locations were assumed to be known and other parameters such as porosity, volume fraction, fracture spacing, variogram parameters and boundary recharge parameters were set at their correct values. The mass extraction and injection rates that drive the response of the model were assumed to be perfectly known.

Model calibration involved identifying the permeability of the faults and the background formation that would reproduce the response obtained from the synthetic model. The background permeability structure was determined using kriging interpolation from 85 pilot points, 4 of which were placed at the well locations while the rest were spaced 1km away from each other. Pilot point interpolation was chosen because it provides the calibration process with the flexibility to put heterogeneity in the permeability if needed (Dohery, 2003). This approach frees the modeller from having to make prior assumptions on the geometry and extent of the region where rock properties are assumed to be equal or similar in value. This procedure, however, also poses a risk of creating a model with a permeability structure that is inconsistent with the known geology of the true system especially if pilot point locations are poorly chosen.

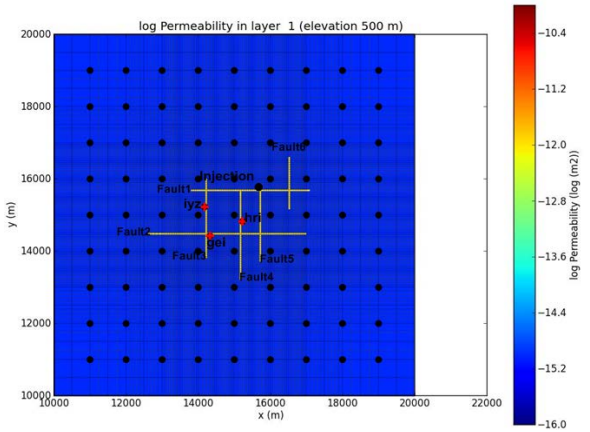

Figure 3. Working model showing the locations of the pilot points and faults.

In modelling a real system, there will be more unknowns than were dealt with in this example. Additionally, the choice of the grid structure will also have an effect on the model's ability to estimate the system properties thereby adding to its potential for error.

3.2 Model Calibration

The calibration was performed automatically using PEST. The initial guess for all the fault fracture permeabilities was 1000mD and the permeability for all the pilot points was set at 1mD. The matrix permeability for both the faults and background rock was set at 1.00E-4 mD. The weights of the observation data were set approximately equal to the standard deviation of the noise used to generate the synthetic response and scaled accordingly to ensure equal visibility of each type of data in the objective function. In practice, these weights may be adjusted as part of the calibration process to get a better match to the data. However, our aim is not to produce the best data fit, but rather to quantify the model uncertainty, and so our weighting scheme is chosen with this in mind. During the calibration process, the logarithm of the permeability was estimated rather than the permeability itself.

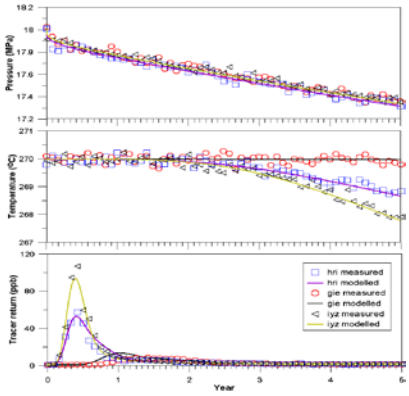

Figure 4. Comparison of the measured data with the modelled response after model calibration

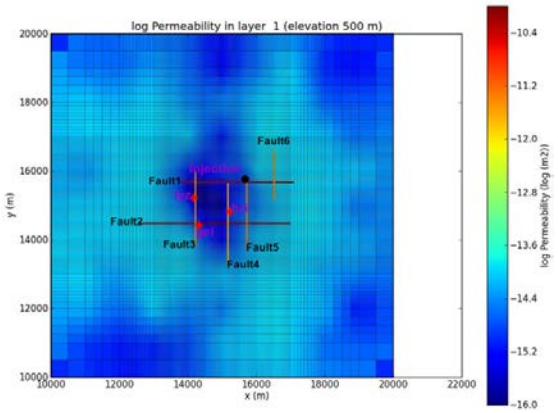

(a)

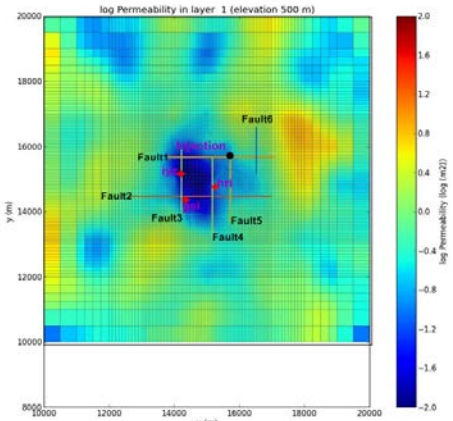

(b)

Figure 5. Permeability distribution of the calibrated model (a) and contour of the difference between the true and working model (b).

The number of parameters involved and the limited data available were expected to make the calibration process difficult. To overcome this problem, one can selectively choose only a few parameters to calibrate based on a sensitivity analysis done prior to the actual calibration as described by (Omagbon and O'Sullivan 2011). For this study however, an automated approach that used Tikhonov regularization was adopted. In this approach, a penalty objective function (or regularization objective function) was added to the total objective function for every deviation of parameter values from its current value. This means that the non-influential parameters, which would have caused calibration difficulty, tend to remain close to their initial values. There was no need to make prior assumption about which parameters to exclude because they were automatically determined after each parameter upgrade.

The result of the calibration is shown in Figure 4 and Figure 5. The temperature, pressure and tracer responses obtained by the calibrated model from the three wells were consistent with the measured data. However, comparison of the permeability for each block obtained after the calibration with that of the true model (Figure 5) shows a significant mismatch (about two orders of magnitude) in the background permeability near the area of the three production wells. This mismatch will be explored further in the succeeding section. Without the knowledge of the true permeability distribution, one would readily conclude that the calibrated model is a good representation of the true system and can be used for prediction purposes.

3.3 Post Calibration Parameter Uncertainty

As previously discussed, the resulting covariance matrix calculated using the gradient information of the model parameters with respect to the data that was used in the calibration process contains an approximation of the uncertainty associated with the parameters around the local solution. The standard deviation (given by the square root of the diagonal component of the covariance matrix) of each of the parameters used in the calibration together with the estimated and true values are shown in Table 1.

Table 1. Results of parameter estimation of the model permeabilities using PEST.

Parameter	Estimated value (m^2)	Standard deviation of (in log scale)	True value (m^2)
fault1	7.67E-11	0.37	1.00E-11
fault2	8.01E-11	0.58	5.00E-12
fault3	3.14E-12	0.08	2.00E-12
fault4	1.66E-12	0.06	1.00E-12
fault5	4.04E-12	0.06	7.00E-13
fault6	3.44E-12	0.58	3.00E-11
matx1	1.65E-17	1.66	1.00E-18
Background	6.44E-15*	0.20 – 283.17	1.18E-14*

* Average value

The high standard deviations correspond to the parameters of the model that cannot be identified with the data that is available. For these cases, using expert knowledge to estimate their values would be better than trying to determine them by calibration. The plot in Figure 6 shows the post calibration standard deviation in permeability for each of the pilot points and faults. The largest circles denote standard deviation higher than 2 or a parameter uncertainty that is about 4 orders of magnitude away from the estimated value. This means that the permeabilities around the region of the large circles were not properly identified by calibration and therefore have higher uncertainty. This is because the observation data used in the calibration does not contain sufficient information to properly estimate those parameters.

Modellers should therefore be cautious in making predictions that are dependent on the permeability of those large circle areas given that the model was not properly constrained at those locations. For example, Fault #6 (the rightmost vertical fault) has a relatively large standard deviation compared to the other faults. This is not surprising because it is located away from where the data were collected and hence it is to be expected that measured data contains little or no information at all about the permeability for this fault. A forecast, for example, involving transferring the injection closer to this fault is likely to result in an increase in uncertainty level. If such a level of uncertainty is not acceptable, then additional data collection activities have to be planned to better characterize the properties of that fault and therefore reduce the uncertainty in its permeability.

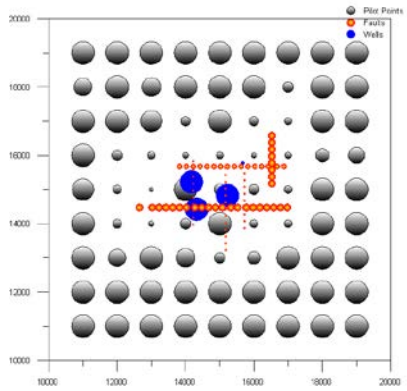

Figure 6. Standard deviation bubble plot of the pilot point and fault permeabilities (log scale). The largest circles denote parameters with standard deviation higher than 2.0.

The pilot points located more than 2 km away from the wells show standard deviation higher than or equal to 2. This is again what one would expect given their distance from the where the data were measured. There were a few pilot points with low standard deviations such as the two at the right hand side of the model (4th row from the top). This is likely to be related to the effect of the pressure dependent recharge blocks at the side of the model on the simulated responses in the wells. Since the boundary recharge is affecting the response of the well, it is required that information about the connection of the boundary blocks and the wells has to be known to some extent.

Interestingly, there were also anomalously large standard deviations at the pilot points near the 3 production wells. If this plot is overlaid with the post-calibration permeability distribution in Figure 5, it can be seen that this area coincides with the low background permeability area near the production wells which is notably inconsistent with the true model. One can therefore say that incorrectly estimating those permeability values was not surprising and is the consequence of the calibration process not being able to determine them from the data available. In that case, the modeler is justified in using their expert knowledge to

assign values they think are more realistic for those pilot points.

3.4 Forecasting

The resulting calibrated models were used to make predictions of the reservoir performance for the next five years. Four scenarios were investigated using each of these calibrated models. More importantly, the uncertainty in each of the scenarios was quantified and analyzed. The scenarios that were investigated are as follows:

1. Retain the current production – injection setup
2. Drill a new production well
3. Transfer injection
4. Transfer injection and drill new production

In all the four scenarios, the pressure and temperature response over the forecast period were generated. In addition, the cumulative steam produced after the 10th year was calculated. In a real modelling exercise, decision making is likely be driven by this total steam production because that is what determines the revenue that can be generated from the implementation of the activities involved in each of the four scenarios. The locations of the new wells for Scenarios 2 to 4 are shown in Figure 7.

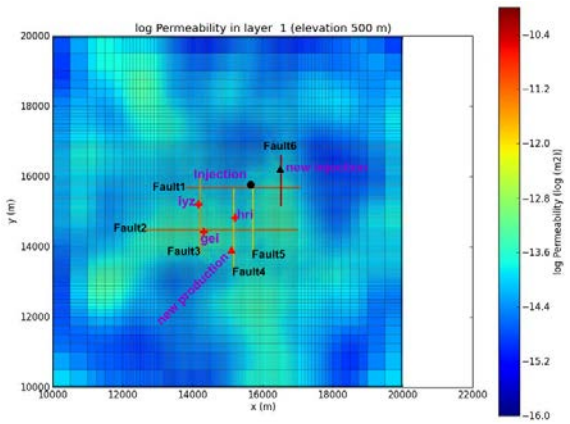

Figure 7. Model grid showing the location of the new production (red triangle) and injection (black triangle) wells used for forecast scenarios 2 to 4.

3.5 Monte Carlo Analysis and Rejection Sampling for Uncertainty Quantification:

In rejection sampling, proposal models are made from some relatively simple parameter distributions. A test is then applied to determine whether or not to accept the proposed models. All samples generated by this method are independent and therefore runs can be made simultaneously. This provides an opportunity for implementing a parallelization algorithm to reduce the time needed to complete the model runs. The key to the efficiency of the rejection algorithm is selecting a proposal density that is a close approximation to the correct posterior probability density function (pdf) of the parameters so that the acceptance rate is close to 100%. It can be difficult to find a simple distribution for the proposal of trial realizations that leads to an efficient sampling, especially when the number of model variables is large. Using the sampling method described in Section 2, samples with a relatively high chance of being accepted can be generated provided the linearity assumption is not severely violated.

A total of 1000 samples were produced using the sampling scheme described in Section 2 (Step iii). Each of the sampled sets of parameters were first tested by checking to see if the weighted least square objective function was low enough for it to be considered as near calibrated. The calibrated model ended up with an objective function value of 117. The rejection criterion was arbitrarily set to an objective function value of 150 so that any model with a higher objective function was discarded. Out of the 1000 samples generated, 630 models with an objective function lower than the threshold were obtained. The reason for the relatively low sampling efficiency is because the uncertainties in some of the parameters were high and therefore samples which are far from the optimized parameters have also been generated making the linear approximation invalid. Nonetheless, the number of accepted models is still reasonably high. Only the forecasts generated by the accepted models were included in the prediction uncertainty assessment.

The resulting responses from the accepted models are shown in Figure 9. There are clear differences in the width of the uncertainty intervals between scenarios. An easier to way interpret the results is by looking at the histogram of the cumulative steam extraction in Figure 8 since this summarizes the effects of the responses from the individual wells. The separation of the distributions effectively quantifies the benefit that can be obtained by selecting one scenario over the other. There is a wide separation between adding and not adding a production well which makes choosing between these two scenarios obvious. However if other factors such as the cost of drilling the well is included in the calculation, the picture might become complicated.

Deciding on whether or not to transfer the injection is more complicated. Under the “no additional production well” scenario (left-side plot in Figure 8), the peak of the distribution suggests that the cumulative steam production will increase if the injection is transferred. This is, however, not guaranteed because the two histograms have significant overlap. If a new production well is drilled (right-side plot of Figure 8), transferring the injection appears to give greater benefit because the separation of the peaks is larger. But again this is not guaranteed because there is a reasonable intersection between the two histograms.

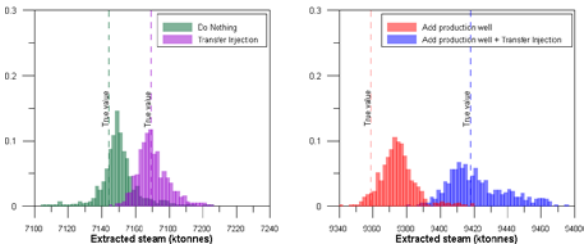

Figure 8. Distribution of the cumulative steam extraction

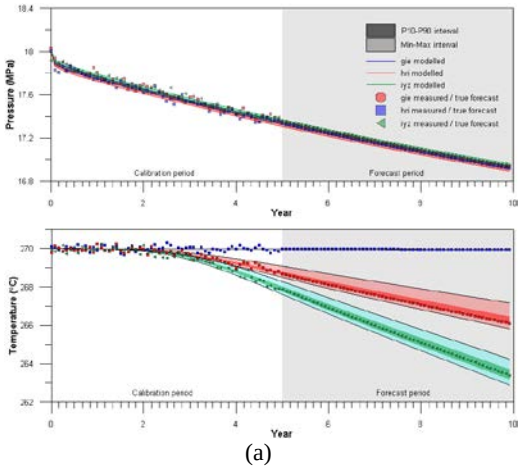

(a)

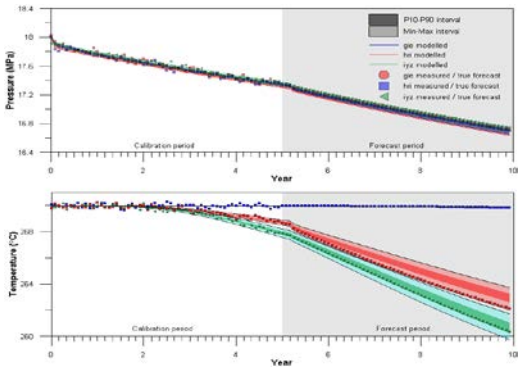

(b)

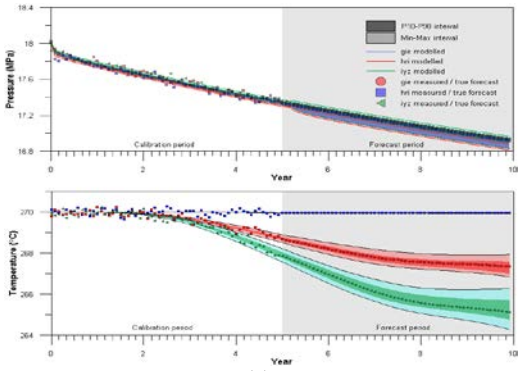

(c)

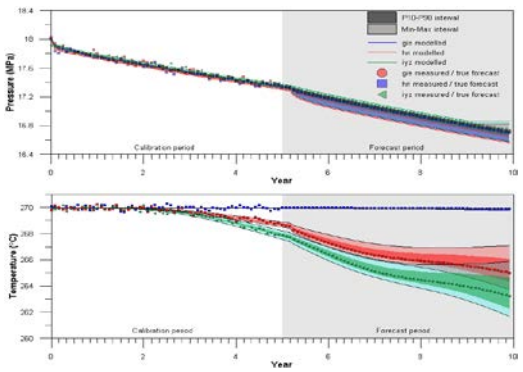

(d)

Figure 9. Forecasted intervals of temperature and pressure for the 3 production wells for scenarios 1 (a), 2 (b), 3 (c) and 4 (d)

3.6 Parameter Contribution to the Uncertainty in the Prediction

Equation (1) in Section 2 provides a cheap way of estimating the uncertainty interval in the prediction because it does not require samples of parameter set to be generated and run to prediction. What is needed instead is the calculation of the forecast gradient matrix J_0. This is easily obtained by making a finite difference approximation on a model that runs through the prediction period. As mentioned earlier, the diagonal elements of the matrix σ^2 corresponds to the variance of each of the predicted quantities and the confidence intervals can be obtained from this if a Gaussian distribution is assumed. In the example described in this paper, this equation was used to estimate the individual parameter contribution to the prediction uncertainty. This was accomplished by calculating how much σ^2 reduces if the row/column corresponding to the parameter of interest is taken out from the J_0 and C_x matrices (Doherty, 2015).

As previously discussed, two of the factors affecting the contribution of a parameter to the uncertainty of a prediction are its influence on the predicted quantity and its uncertainty. Figures 10 and 11 show the individual contributions of the parameters to the uncertainty of the cumulative steam production for scenarios 1 and 4 as estimated using Equation (1). In this plot, larger circles indicate higher contribution. Both plots were set to have the same minimum and maximum values so they can be compared with each other. Information like this can be useful in identifying which parameters are crucial in making certain predictions.

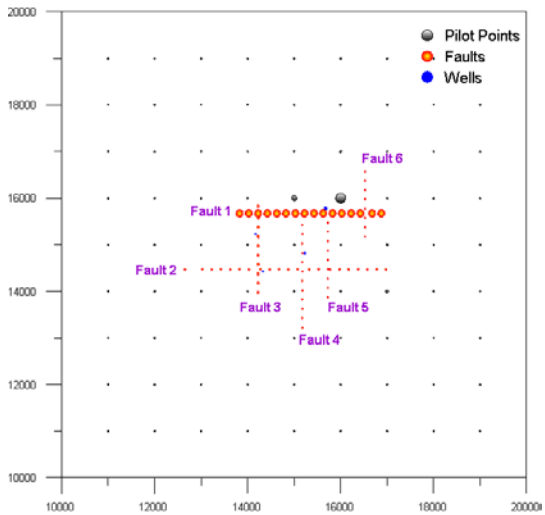

Figure 10. Contribution of the permeability of the pilot points and faults to the uncertainty of the predicted cumulative steam production for Scenario 1.

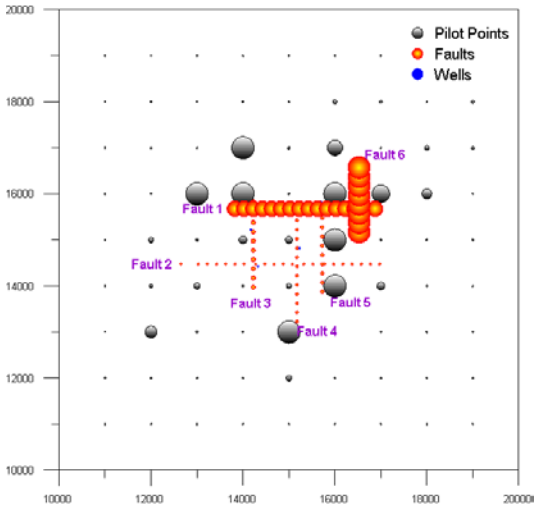

Figure 11. Contribution of the permeability of the pilot points and faults to the uncertainty of the predicted cumulative steam production for Scenario 4.

For Scenario 1, the prediction is sensitive to the parameters whose uncertainties were significantly reduced during the calibration. This explains why all the parameters contribute little to the uncertainty in the predicted cumulative steam production. In Scenario 4, the operating conditions are different from that of the calibration period therefore the influence of the parameters to the cumulative steam production changes. As can be seen from Figure 11, the faults and some of the pilot points near the wells now have higher contribution to the uncertainty. Fault 6 contributes significantly because the new injection well is located near it (making the prediction sensitive to it) in addition to having a high uncertainty value. The prediction is likely to be just as sensitive to Fault 1 as it is to Fault 6. But since the uncertainty in Fault 1 is smaller, it has a smaller contribution than Fault 6.

4. SUMMARY AND CONCLUSION

This work demonstrated a synthetic case of predictive uncertainty quantification in reservoir simulation using a calibrated model and the local gradient information. The key to making a reliable prediction from a geothermal model is the accurate identification of the parameters that affects the model's response. The post calibration parameter uncertainty gives an indication of how well these parameters were identified given the amount of data used for the calibration. Consequently, this gives modelers a means to assess how reliably a forecast can be made from the model. By using local gradient information, several models with relatively low objective function can be generated efficiently and used to investigate different model outcomes. Using this set of models, the different levels of uncertainty of predictions on different scenarios was quantified. Such information can also be used in determining which parameters are causing the uncertainty.

The approach presented here does not account for all the sources of uncertainty especially, those from structural and numerical errors. It is also likely to underestimate the uncertainty especially for highly nonlinear models with many local minima and non-Gaussian parameter distribution. While better methods are needed to address these issues, this technique is still particularly useful in geothermal modeling. This is mainly because at present, operators likely have an existing model in place, calibrated by some standard method, which they use for making deterministic future predictions. With a little more effort, this method provides useful information which is not usually available to the reservoir engineers and decision makers.

ACKNOWLEDGEMENTS

The authors appreciate the financial support of Energy Development Corporation, the New Zealand Ministry of Business, Innovation and Employment, and the Energy Education Trust of New Zealand.

REFERENCES

Arras, K. O.: *An introduction to error propagation: derivation, meaning and examples of equation CY = FX CX FXT*. Lausanne. Swiss Federal Institute of Technology Lausanne (EPFL); Report nr EPFL-ASL-TR-98-01 R3. (1998).

Beven, K., & Binley, A.: The future of distributed models: Model calibration and uncertainty prediction. *Hydrological Processes*, 6, 279-298. (1992).

Devore, J.: *Probability and statistics for engineering and the sciences* (2nd ed.). Belmont, California: Brooks/Cole Publishing Company. (1987).

Doherty, J.: *Calibration and uncertainty analysis for complex environmental models* (1st ed.). Brisbane, Australia: Watermark Numerical Computing. (2015).

Doherty, J.E., Hunt R.J.: *Approaches to highly parameterized inversion: a guide to using PEST for groundwater-model calibration*. US Geological Survey Report, (2010).

Doherty JE, Hunt RJ and Tonkin MJ: *Approaches to highly parameterized inversion: a guide to using PEST for model-parameter and predictive-uncertainty analysis*. US Geological Survey Scientific Investigations Report. (2010).

Doherty, J.: Ground water model calibration using pilot points and regularization, *Ground Water*, 41(2), 170–177. (2003).

Finsterle, S.: *iTOUGH2 user's guide*. LBNL-40040. (1999).

Iman, R. L., & Conover, W.: A distribution-free approach to inducing rank correlation among input variables. *Communications in Statistics-Simulation and Computation*, 11(3), 311-334. (1982).

Kalogerakis, N.: An efficient procedure for the quantification of risk in forecasting reservoir performance. *Society of Petroleum Engineers*. doi:10.2118/27569-MS. (1994).

Lepine, O. J., Bissell, R. C., Aanonsen, S. I., Pallister, I. C., & Barker, J. W.: Uncertainty analysis in predictive reservoir simulation using gradient information. doi:10.2118/57594-PA. (1999).

Moon, H., Clearwater, J., Franz, P., Wallis, I., & Azwar, L.: Sensitivity analysis, parameter estimation and uncertainty propagation in a numerical model of the Ngatamariki geothermal field, New Zealand. *Stanford Geothermal*

Workshop, Stanford University, Stanford, California. (2014)

Oliver, D. S., Reynolds, A. C., & Liu, N.: *Inverse theory for petroleum reservoir characterization and history matching*. Cambridge University Press. Cambridge. (2008).

Omagbon, J.B., & O'Sullivan, M.J.: Use of a heuristic method and PEST for calibration of geothermal models. *Proc. 33rd New Zealand Geothermal Workshop*, Auckland, New Zealand. (2011).

Tarantola, A.: *Inverse problem theory: methods for data fitting and model parameter estimation*, pp. 500, Elsevier Sci., New York. (1987).

Tureyen, O. I., & Onur, M.: Assessing uncertainty in future performance predictions of lumped parameter models using the randomized maximum likelihood method. *World Geothermal Congress*, Bali Indonesia. (2010).

Vogt, C., Marquart, G., Kosack, C., Wolf, A., & Clauser, C.: Estimating the permeability distribution and its uncertainty at the EGS demonstration reservoir Soultz-sous-Forêts using the ensemble Kalman filter. *Water Resources Research*, 48(8), doi:10.1029/2011WR011673: (2012)